Recent Advancement of Research on Plasma Direct Energy Conversion[*]

Hiromasa TAKENO, Kazuya ICHIMURA, Satoshi NAKAMOTO,
Yousuke NAKASHIMA[1], Hiroto MATSUURA[2], Junichi MIYAZAWA[3],
Takuya GOTO[3], Yuichi FURUYAMA[4] and Akira TANIIKE[4]

Graduate School of Engineering, Kobe University, Kobe 657-8501, Japan
[1]*Plasma Research Center, University of Tsukuba, Tsukuba 305-8577, Japan*
[2]*Radiation Research Center, Osaka Prefecture University, Sakai 590-8570, Japan*
[3]*National Institute for Fusion Science, Toki 509-5292, Japan*
[4]*Graduate School of Maritime Sciences, Kobe University, Kobe 658-0022, Japan*

Present plasma direct energy conversion (DEC) system has been developed since proposal of ARTEMIS. The system for D-^{3}He reactor is composed of cusp-type DEC (CuspDEC) for particle discrimination, traveling wave DEC (TWDEC) for recovery of high energy protons, and secondary electron DEC (SEDEC) for recovery of extremely accelerated protons. Studies on each device are in the third stage, where higher capability of each device will be derived. Various proposals and examinations were reported and the present paper treats the researches comprehensively and shows explanation and discussion for some researches: separation of high density plasma and ion-ion separation in CuspDEC, studies on modulation in TWDEC, and improvement of electron collection in SEDEC.

1. Introduction

The first study of plasma direct energy conversion (DEC) was that by Moir, et al. [1], however, recent studies have an origin in the proposal of ARTEMIS [2]. A pair of sets of cusp-type direct energy converter (CuspDEC) and traveling wave direct energy converter (TWDEC) are placed at both ends of an FRC-based D-^{3}He fusion reactor. Charged particles flowing out from the reactor are discriminated in the CuspDEC composed of 2-stage cusp field without any grid electrodes. Electrons and thermal ions are deflected to line cusp regions of the first and the second stage cusp fields, respectively, and recovered by conventional electrostatic energy converters, such as a Venetian-blind type converter. High energy fusion-produced protons are passing through the cusp fields, and recovered by the TWDEC, which works based on the principle of the inverse process of a linear accelerator. The proton beam is velocity-modulated in the modulator, and density-modulated in the downstream. The bunched protons are trapped in the potential valley of traveling wave in the decelerator, and decelerated with the traveling wave.

Following to the proposal of ARTEMIS, various studies were reported. The proposals concerning to system structure are summarized in Fig. 1. As for CuspDEC,

one slanted cusp field was proposed instead of 2-stage one [3]. A simulator with a slanted cusp was constructed and more efficient separation was shown than a normal cusp. The simulator also succeeded in lighting demonstration on GAMMA 10 [4]. In relation to TWDEC, secondary electron direct energy converter (SEDEC) was proposed [5]. As TWDEC works according to inverse process of a linear accelerator, some out-of-phase protons are not decelerated, but accelerated. The energy of those protons is enormous, so they can penetrate foil electrodes and cause secondary electrons to be emitted. The device with a lot of foil electrodes is installed at the bottom of the conversion system as in Fig. 1.

On one hand, the concept of CuspDEC was applied to divertor problem [6]. Plasma flowing into divertor plate was previously separated by a cusp field, and the electric field by divertor plates appropriately biased according to charged particles flowing in could reduce particle energy, and thus thermal load. For actual application in a narrow divertor space, CuspDEC composed of permanent magnet (PM-CuspDEC) was proposed [6], and basic research has been continuing [7, 8].

To realize DEC system of Fig. 1 and other applications, various researches to derive higher capability of each device are ongoing. In this paper, we pick up some unpublished works, and show in detail with discussion.
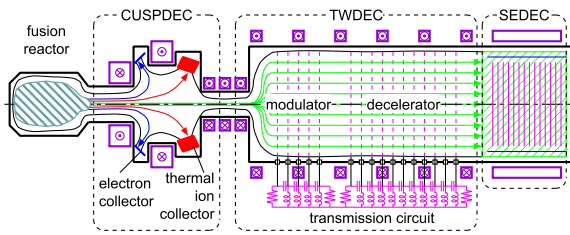
Fig. 1   Proposed structure of DEC system.

Fig. 2   Structure of the CuspDEC simulator.

Two researches on CuspDEC in Sec. 2, two researches on TWDEC in Sec. 3, and one research on SEDEC in Sec. 4 are presented. The contents of the paper are summarized in Sec. 5.

2. Studies on CuspDEC

The most essential function of the CuspDEC is to separate charged particles. Effective separation provides high power conversion efficiency, and a typical example was shown in the study of two-stage deceleration [9]. Separation in particle energy enables precise setting of retarding bias voltage of the collector, and results in high conversion efficiency. Introduction of two-stage deceleration improves energy recovery of thermal ions over 10%, and the overall efficiency of CuspDEC is estimated to be 65% [9]. In the following, studies on ion-electron separation and ion-ion separation are shown.

2.1   Separation assistance for high density plasma

Ion-electron separation was well studied, and a problem was pointed out that separation capability degraded on the application to high density plasma [10]. Some additional means are required for separation of high density plasma.

As an additional mean, non-linear effect of radio frequency (RF), i.e. pondermotive effect was proposed and a basic phenomenon were studied [11]. In a CuspDEC simulator shown in Fig. 2, repetitively pulsed plasma was incident into the cusp field. A pair of RF electrodes of ring shape are aligned in the line cusp, to which in-phase RF voltage is applied during plasma pulse. A reaction of plasma to RF application was found [11], however, orbit calculation suggested the reaction was not due to non-linear effect, but linear effect.

In the following study using the same experimental setting as Ref. [11], a curious phenomenon was found. Its sample is shown in Fig. 3. The signals are currents of the electron collector in the line cusp (I_e). In the upper trace (the frequency of RF is 11 MHz), electron current increases by 50 - 60% on the application of RF. However, the increasing ratio becomes around 800% on the frequency of 13 MHz in the lower trace. The change of the reaction was discontinuously found to the change of frequency and volt-
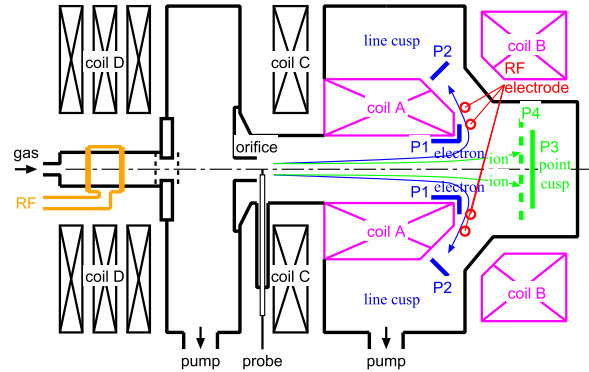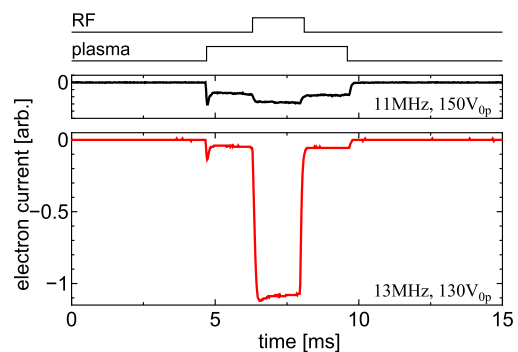

Fig. 3   Sample waveform of electron collector current on the application of RF in the line cusp.

age amplitude. Those are summarized in Fig. 4. In the frequencies from 6 to 11 MHz of Fig. 4 (a), increasing ratio of electron current (I_e/I_{e0}; I_{e0} is the electron current without RF) gently changes as the RF voltage amplitude changes. On the other hand, in the range over 12 MHz of Fig. 4 (b), I_e/I_{e0} changes abruptly over the amplitude of 100 - 120 V_{0p}.

Although possible cause of the phenomenon, such as RF noise or discharge by RF was investigated, it was not clarified yet. As the phenomenon is an increment of electron current of the electron collector, it is favourable for the charge separation.

2.2   Ion-ion separation

Although ion-electron separation has been studied well, studies on ion-ion separation are few. In the original proposal of CuspDEC, this function was realized by another strong cusp field. We newly propose separation by electric field, which is conceived by two-stage deceleration studied in the past [9].

Ions with different energies are necessary to perform an ion-ion separation experiment. We are proceeding construction of a combined plasma source as well as a separation experiment itself. Figure 5 shows total view of the experimental device. The combined plasma source is in-
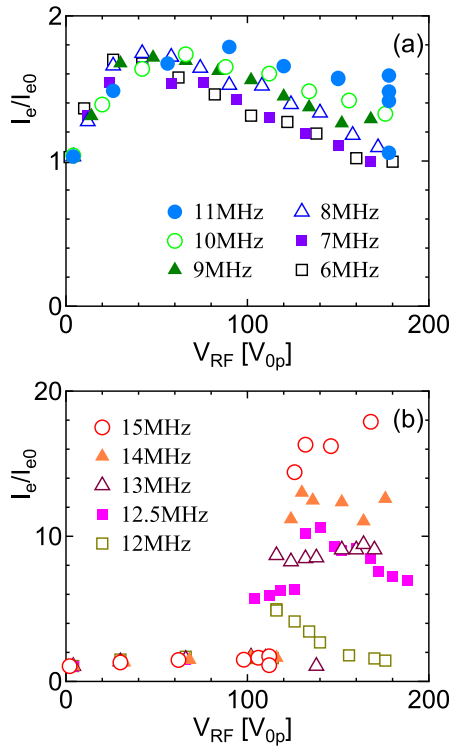
Fig. 4   Increasing ratio of electron current for (a) 6 - 11 MHz and (b) 12 - 15 MHz.
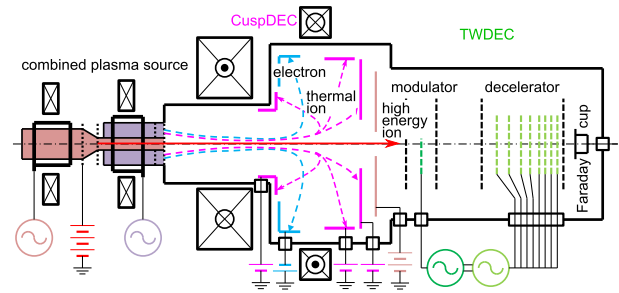

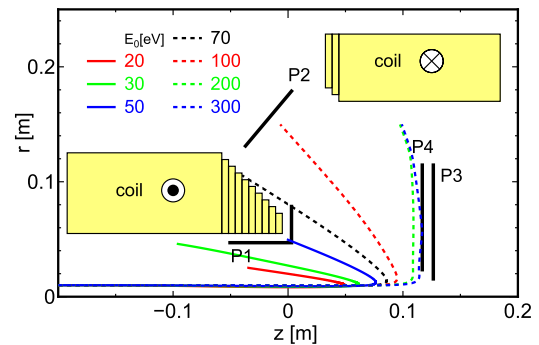Fig. 5   Experimental setting for studies on ion-ion separation.

Fig. 6   Results of orbit calculation for proposed ion-ion separation scheme.
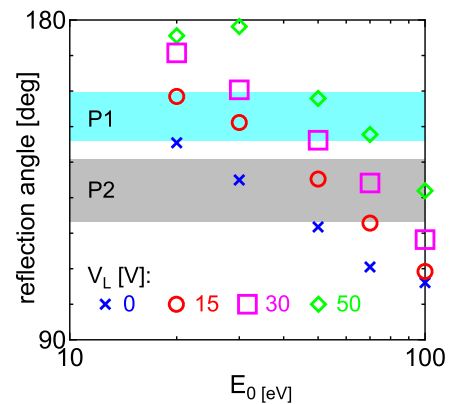

Fig. 7   Reflection angle versus incident energy of ions for several cases of V_L.

stalled in the left of the figure. It has two independent plasma/ion sources excited by RF, and they are coaxially arranged in series. The upstream source provides fast ions appropriately accelerated by high voltage, and the downstream one provides low energy thermal plasma. The thermal plasma source has a hollow structure, and fast ions of the upstream source will run in the center of the downstream source. Both ions and plasma are mixed in the downstream chamber. The working characteristics of the combined plasma source were reported in the separate presentation [12].

As for ion-ion separation itself, we newly propose the following scenario. The plasma incident in the chamber will arrive a slanted cusp field. Electrons are deflected to the line cusp by magnetic field, and ions go to the point cusp. In the newly proposed ion-ion separation scheme, a pair of disk electrodes with a hole are placed in the point cusp as shown in Fig. 5. When high voltage is applied to the electrode in the downstream, high potential seeps out around the hole of the upstream electrode. High energy ions pass through the holes, but low energy ions are reflected by electric field, thus ion-ion separation will be achieved. High energy ions passing through the CuspDEC are recovered by TWDEC in the downstream. As for reflected low energy ions, dc-biased collectors are used for recovery. This is the same as recovery of low energy ions in the two-stage deceleration [9].

In this scheme, the reflected direction of low energy

ions is various as shown in Fig. 5. The direction depends on incident radial position and energy. Moreover, retarding voltage of the collector affects the trajectory of ions. Here, we show a sample examination by orbit calculation. Figure 6 shows results of orbit calculation in the present CuspDEC simulator shown in Fig. 2. The bias voltages of downstream and upstream disk electrodes (P3, P4) in the point cusp are 800 V and 0 V, respectively, and that of the low energy ion collector at the entrance (P1) is $V_L = 50$ V. Ions are incident at $(r, z) = (0.01$ m, -0.2 m$)$. Curves in the figure show trajectory of ions with incident energy showing by the legends in the figure. In this condition, the ion

with 50 eV is reflected in the direction of P1 and collected. For ions with other energies, the reflection angles are not appropriate for collection by P1.

The relation between ion energy and reflection angle (between positive z direction and reflected direction) was investigated for several cases of V_L. The results are summarized in Fig. 7. Zones indicated by 'P1' and 'P2' express prospect angles of the ion collector P1 and the line cusp electron collector P2 (shown in Fig. 6). For collection of thermal ions with ~30 eV, biasing with $V_L = 15$ V is appropriate. Experiments based on this estimation will be performed in the present CuspDEC simulator.

3. Studies on TWDEC

The most important subject on TWDEC is improvement of energy conversion efficiency. As an example, an actual efficiency about 55% was obtained by two-dimensional numerical simulation [13]. In simulation experiments, two processes of induction of traveling wave and particle deceleration by traveling wave have to be studied separately because of small beam current. Although it is a part of actual efficiency, deceleration efficiency directly affects the actual efficiency. An introduction of constant deceleration scheme greatly improved efficiency [14]. In the scheme, bunching by modulation is important for high efficiency, so studies on the modulation process are also important. On one hand, there is a significant trade-off between device size and bunching, and thus efficiency [15]. It relates to modulation as well as deceleration processes. Two studies on modulation process are presented in the following.

3.1 Delay of modulation effect

Simulation experiments were usually performed with a repetitive-pulsed operation, and a modulation RF was also applied pulsively. In such experiments, delay of modulation effect was observed [16].

Figure 8 shows a typical setting for a modulation experiment in TWDEC. Helium plasma is excited by 1 kHz repetitive pulsed RF. Helium ions are extracted from the
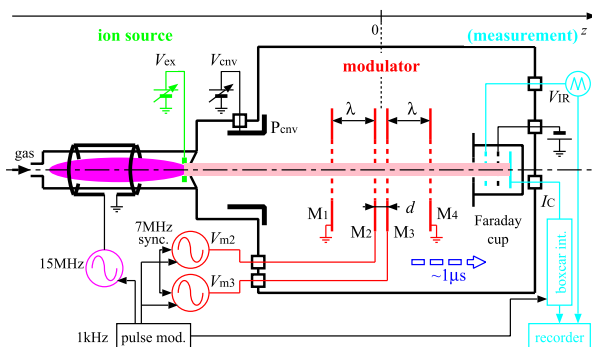
plasma source by extraction voltage $V_{ex} = 3.7$ kV, and converged by convergence voltage $V_c = 0.5$ kV. The running time of ions in the device is on the order of 1 μs. Phase controlled synchronous two RF voltages of $f = 7$ MHz are applied to electrodes M_2 and M_3 for modulation (V_{m2} and V_{m3}, respectively), while M_1 and M_4 are grounded. By taking an appropriate phasing between RF sources and an appropriate distance between M_2 and M_3 (d), the field between M_2 and M_3 is that of traveling wave. The fields between M_1 and M_2 and between M_3 and M_4 are those of standing wave, and the effects are negligible by taking those distances with $\lambda = v_0/f$, where v_0 is ion velocity corresponding to energy of eV_{ex} (e is elementary charge). The energy of the modulated beam is analyzed by a Faraday cup.

Time resolved energy distribution of the beam was measured as shown in Fig. 9. Each time is as shown in the figure, where the origin of time is start of plasma and modulation voltage starts at 180 μs. The incident energy of ions is 3.9 keV, which is a result of adding ~200 eV due to space potential of the plasma in the source. The modulation effect is confirmed by increase of tail components in the side of the incident energy. According to Fig. 9 (a) of $V_{m2} = V_{m3} = 80$ V$_{0p}$, the components of 3.6 - 4.2 keV increase as time elapses. In the case of Fig. 9 (b) of $V_{m2} = V_{m3} = 190$ V$_{0p}$, the components of 3.4 - 4.4 keV increase in the same way with a time constant on the order of 100 μs. The response time of the beam is considered to be determined by modulation frequency and/or ion running time in the device, and is expected to be within a few micro-seconds. The long time constant suggests some

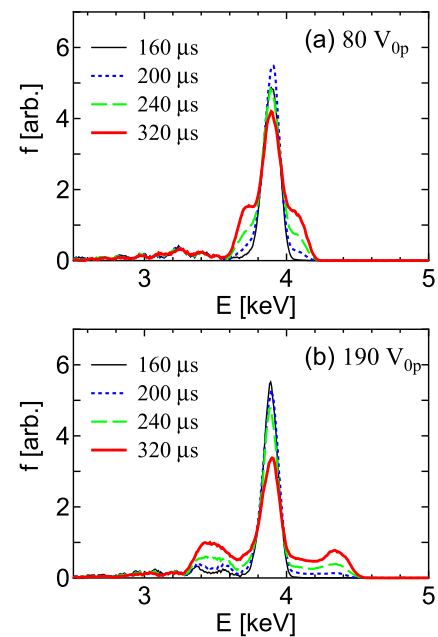Fig. 8   Typical setting for modulation experiment in TWDEC.

Fig. 9   Time variation of energy distribution function of RF modulated ion beam.
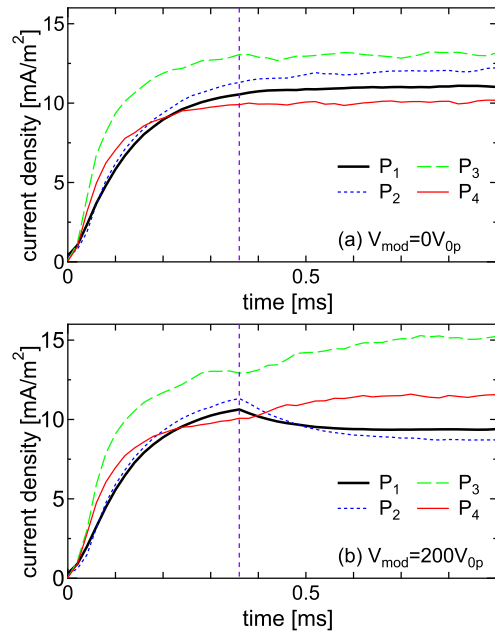
Fig. 10 Examples of evolution of radially segmented electrode currents.

Fig. 11 Variation of time constant to radial position and modulation voltage.

other effects concern in the simulation experiment.

3.2 Observation of scattering

The proton beam is guided into TWDEC with spatial expansion as in Fig. 1, so space potential by protons is not significant. However, protons are density modulated and bunched, where significant potential may be created by high density proton. In the previous numerical report, radial scattering of ions based on this mechanism was predicted [17]. Later, the corresponding phenomenon was found in the experiments.

In the similar setting to Fig. 8, the Faraday cup was replaced by an array of radially 4-segmented electrodes. The modulator was simplified that RF voltage V_m was applied to one electrode, and uniform fields in the front and rear regions of the electrode were used for modulation. The convergence voltage was changed to control the beam density under $V_{ex} = 3.2$ kV.

Figure 10 shows samples of electrode currents when the density of the beam is appropriately high on $V_c = 400$ V. No modulation voltage was applied in Fig. 10 (a), where the currents are stable after 0.35 ms of the start of the plasma. When $V_m = 200\,V_{0p}$ was applied after 0.35 ms in Fig. 10 (b), electrode currents changed that those of inner electrodes (P_1 and P_2) decrease while those of outer electrodes (P_3 and P_4) increase. The relative increment of outer current means radial scattering. The phenomenon was examined about dependence on V_c and V_m, and the results were consistent with radial scattering on bunching [18].

According to Fig. 10 (b), time constants on the order of 0.1 ms can be observed in the change of current by modulation. They were evaluated and summarized in Fig. 11,
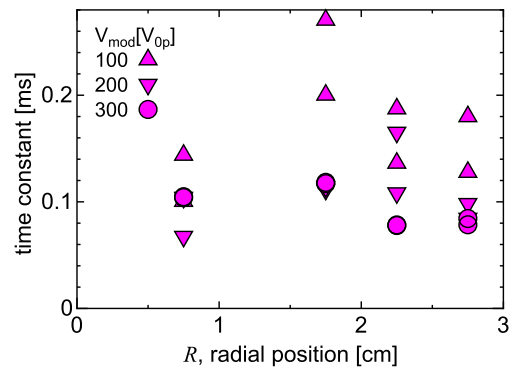
where the abscissa means average radius of the electrode. Although the time constant varies according to the conditions, it is in the range of 0.06 - 0.27 ms and this is in the same order as that of delay of modulation effect explained in the previous subsection. The reason of the time constant of the scattering is under discussion, but some relation between delay of modulation effect and radial scattering is expected.

4. Studies on SEDEC

As TWDEC is based on the inverse process of a linear accelerator, some protons incident in TWDEC are accelerated and flow out of the TWDEC. Secondary electron (SE) direct energy converter (SEDEC) was proposed to recover those accelerated protons [5]. Its principle is illustrated in Fig. 12. The accelerated protons are guided to the SEDEC, where a lot of foil electrodes are aligned in the direction of the proton beam. As the energy of the protons is high enough, they can penetrate the foils, when SEs are emitted. The electron collectors are on the side of the foils, and emitted SEs are collected and recovered by appropriately biased collectors. Thus, the energy of protons is recovered indirectly. The present estimation of the efficiency of SEDEC is 1% (energy of secondary electrons is 10^{-5} of that of protons, and a single proton emits 10 electrons from one foil while the proton can penetrate 100 foils), but improvement of 1% in a huge power system is significant.

Some studies were following to the proposal of SEDEC by using fast protons accelerated by a tandem electrostatic accelerator [5, 19]. In a basic structure of SEDEC, many emitted SEs were not incident to collectors, but anterposterior foil electrodes. To limit electron's motion, magnetic field perpendicular to the beam direction was applied by permanent magnets as shown in Fig. 13. SEs incident to anterposterior electrodes decreased, however, SEs arriving at collectors did not increase. The field structure in front of the collectors was magnetic mirror, so SEs were reflected before the collector. Some improvements were shown, but their effects were limited [19].
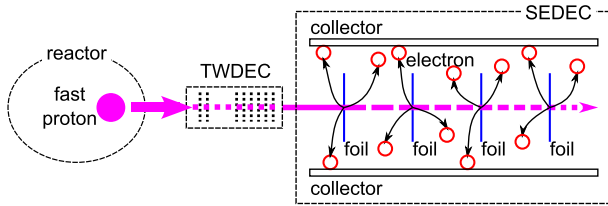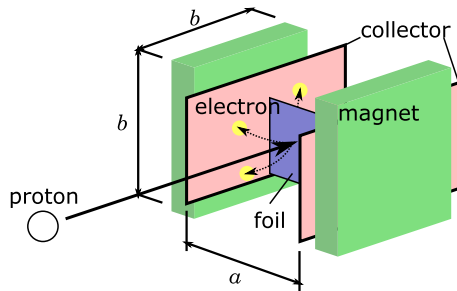
Fig. 12 Illustration of principle of SEDEC.

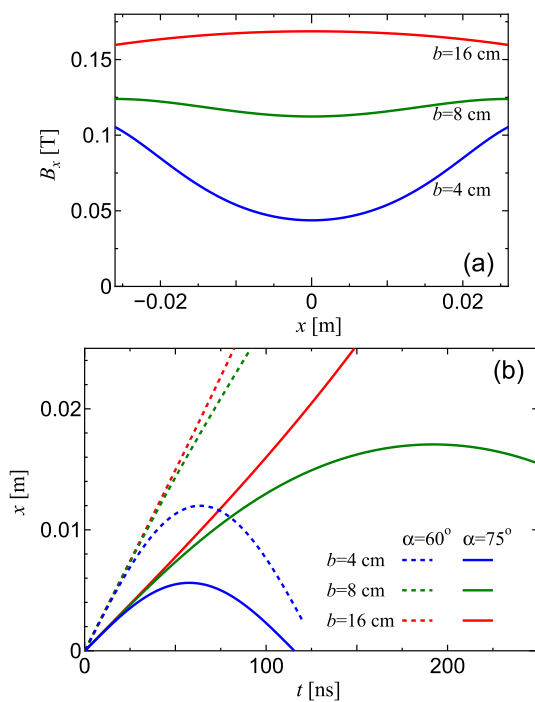Fig. 13 Usual structure of SEDEC with permanent magnets.

Fig. 14 Results of orbit calculation in the magnetic structure of SEDEC. Here, (a) and (b) show field distribution and trajectory of electrons, respectively.

We propose a radical solution to the problem. In the usual structure shown in Fig. 13, field strength is distributed in a valley shape between collectors. When we use large size magnets with $b > 2a$, the field between collectors becomes a hill shape, which can be suggested from relation between distance and diameter of Helmholtz coils.

The above idea was confirmed by numerical orbit cal-

culation. The permanent magnets were modeled by a number of magnetic dipole arrays, and the motion of a single electron in the magnetic field was calculated. Three cases: 4, 8, and 16 cm were taken as the size of b in Fig. 13 with taking $a = 5$ cm. As for initial pitch angles, two cases of 60 and 75 degrees were examined.

The results are shown in Fig. 14. Figure 14 (a) shows distribution of magnetic field between collectors. For $b = 4$ and 8 cm, fields are in valley shapes, but it becomes a hill shape for $b = 16$ cm. SE's trajectories are shown in Fig. 14 (b). According to the figure, SEs of both initial pitch angles are reflected for $b = 4$ cm, while that of 60 degrees arrives at the collector for $b = 8$ cm. For $b = 16$ cm, however, both SEs arrive at the collector, thus our proposal can be expected to solve the mirror effect problem.

5. Summary

Various studies on plasma direct energy conversion are in the third stage deriving higher capability of each device. Extreme increment of electron collector current was found by RF field application in charge separation experiment of CuspDEC. Studies on ion-ion separation in CuspDEC are in progress for development of a combined plasma source and proposition of a new scheme of ion-ion separation by electric field. In TWDEC, delay of modulation effect was found, and some relation with beam scattering phenomenon by bunching was suggested in terms of time constant of variation. A radical solution to mirror reflection problem in SEDEC was proposed and its effectiveness was confirmed by orbit calculation. The total power conversion efficiency of DEC system is estimated to be about 60% by assuming a similar power flow of ARTEMIS-L [20]. The improvement of capability of each device has a possibility to enhance the power conversion efficiency.

Acknowledgments

[1] R.W. Moir and W.L. Barr, Nucl. Fusion **13**, 35 (1973).
[2] H. Momota *et al.*, Proc. 7th Int. Conf. on Emerging Nucl. Energy Systems, 16 (1993).
[3] H. Takeno *et al.*, Trans. Fusion Sci. Tech. **39**, 386 (2001).
[4] Y. Yasaka *et al.*, Nucl. Fusion **48**, 035015 (2008).
[5] D. Akashi *et al.*, Trans. Fusion Sci. Tech. **63**, 301 (2013).
[6] H. Takeno *et al.*, Trans. Fusion Sci. Tech. **63**, 131 (2013).
[7] Y. Nonda *et al.*, Plasma Fusion Res. **13**, 3405050 (2018).
[8] K. Ichimura *et al.*, Fusion Eng. Des. **136**, 381 (2018).
[9] Y. Yasaka *et al.*, Trans. Fusion Sci. Tech. **55**, 1 (2009).
[10] Y. Munakata *et al.*, Plasma Fusion Res. **7**, 2405071 (2012).

[11] M. Hamabe *et al.*, Plasma Fusion Res. **11**, 2405028 (2016).

[12] Y. Okamoto *et al.*, 12th Int. Conf. on Open Magnetic Systems for Plasma Confinement, P16 (2018).

[13] M. Ishikawa *et al.*, Fusion Eng. Des. **41**, 541 (1998).

[14] Y. Togo *et al.*, Plasma Fusion Res. **10**, 3405013 (2015).

[15] H. Takeno *et al.*, Trans. Japan Soc. for Aeronautical and Space Sci., Aerospace Tech. Japan **14**, Pb_105 (2016).

[16] H. Takeno *et al.*, 10th Joint Convention of Fusion Energy, 20-130 (2014).

[17] K. Nishimura *et al.*, Trans. Fusion Sci. Tech. **63**, 310 (2013).

[18] H. Takeno *et al.*, Plasma2017, 24P-91 (2017).

[19] S. Nakamoto *et al.*, Fusion Sci. Tech. **68**, 166 (2015).

[20] H. Momota *et al.*, Proc. 14th Int. Conf. Plasma Phys. and Controlled Nucl. Fusion Res. **3**, 319 (1993).